minerals

MDPI

Article

Content and Forms of Radioactive Elements in Orthite (Allanite)

Victor Ivanovich Sachkov [1], Roman Andreevich Nefedov [1], Rodion Olegovych Medvedev [1], Ivan Vyacheslavovich Amelichkin [1], Anna Sergeevna Sachkova [2], Pavel Sergeevich Shcherbakov [1,*], Vladislav Sergeevich Solovyev [1], Daniil Igorevich Leonov [1] and Danil Aleksandrovich Biryukov [2]

[1] Laboratory of Chemical Technology, Faculty of Chemistry, National Research Tomsk State University, 634050 Tomsk, Russia
[2] School of Nuclear Science & Engineering, National Research Tomsk Polytechnic University, 634050 Tomsk, Russia
* Correspondence: xcrbgc@gmail.com

Abstract: The present work analyzes the specimens of orthite (allanite) mineral ores obtained from the Vernadsky mine (Slyudyanka River, Irkutsk region) and Yuzhno-Bogatyrskoye occurrence (Kuznetsk Alatau). The elemental chemical composition of the ore was determined by electronic microscopy of the specimen's surface. The study establishes that uranium and thorium in orthite ores of the Yuzhno-Bogatyrskoye occurrence are mainly represented by their separate minerals, while the content of the orthite phase in the form of their isomorphic inclusion is small.

Keywords: orthite; mineral; radioactive elements; uranium; thorium

check for updates

Citation: Sachkov, V.I.; Nefedov, R.A.; Medvedev, R.O.; Amelichkin, I.V.; Sachkova, A.S.; Shcherbakov, P.S.; Solovyev, V.S.; Leonov, D.I.; Biryukov, D.A. Content and Forms of Radioactive Elements in Orthite (Allanite). *Minerals* **2023**, *13*, 366. https://doi.org/10.3390/min13030366

Received: 23 November 2022
Revised: 16 February 2023
Accepted: 22 February 2023
Published: 6 March 2023

Copyright: © 2023 by the authors. Licensee MDPI, Basel, Switzerland. This article is an open access article distributed under the terms and conditions of the Creative Commons Attribution (CC BY) license (https://creativecommons.org/licenses/by/4.0/).

1. Introduction

Orthite (allanite) is a mineral of the epidote group or complex silicates of calcium, aluminum and iron. The common formula is $A_2M_2Si_3O_{12}[OH]$, where A is a cation of Ca^{2+} or Sr^{2+} and rare-earth elements (REEs); M is Al^{3+}, Fe^{3+}, Mn^{3+}, Fe^{2+}, Mg^{2+} or other [1]. Another formula of orthite or hydrosilicate of REEs can be $(La, Ca)_2(Al, Fe)_3Si_3O_{12}(O, OH)$ [2].

Orthite in ores can also represent both disseminated crystals and veins of various widths, ranging from several millimeters to some meters. An orthite grain is black, having a submetallic luster, uneven surface and average roundness [3]. The maximum content of rare-earth elements (REEs) in allanite, as a rule, is 5% of rare-earth oxides; however, for some sources, it can vary from 3 to 51%. The content of thorium is also different: ranging from traces to up to 3% [4]. Uranium often is not detected as an inclusion.

The reason for the radioactivity of REE minerals, in particular allanite, is the similarity of Th, U and REE behavior in endogenous processes [5]. The similar structure of the outer electron shells of U, Th, and REE is responsible for the common patterns of their behavior in natural processes and their lithophilicity. The proximity of the ionic radius of these elements causes their isomorphism in minerals. Thorium is closest to cerium, samarium, neodymium and gadolinium, with which it is associated in high-temperature deposits. Joint occurrence of thorium, uranium and rare-earth elements in endogenous processes is also predetermined by the fact that they have a common analogue among petrogenic elements, such as calcium, whereas calcium minerals are the main carriers of these elements. The incorporation of uranium and thorium in calcium minerals depends largely on the presence of rare-earth elements in them. As is known, all high-temperature rare-earth accessory minerals of pegmatites (monazite, orthite, titanium-tantal-niobates) are constantly enriched in thorium and uranium. As the temperature decreases in the postmagmatic stage, thorium, uranium and rare-earth elements are separated due to changes in the acid-alkali characteristic of the process.

The concentration of rare-earth elements exceeds the corresponding clarks 50–80 times in uranium-bearing pegmatites. Pegmatites are characterized by the division of rare-earth elements into two separate groups: cerium and yttrium. In this case, uranium is usually associated with the elements of the yttrium group, and torpy is related to the elements of the cerium group. A small portion of uranium and thorium falls to the share of rock-forming minerals. Uranium concentrations are usually estimated at thousands, more rarely at hundreds, and in some cases at tenths of a percent per mass of the pegmatite vein.

The regularities of allanite radioactivity are also described in [6]. For example, more altered portions of allanite are noted to be less radioactive than the unaltered ones. This indicates a higher migration ability of uranium and thorium than that of REE, including leaching the radioactive elements during alteration.

The high-level radioactivity of allanite of the Kavala pluton is stated in [7]. Thorite, monazite and magnetite were identified as inclusions in allanite. Allanite is also noted to be present in the magnetic and non-magnetic fractions, which the authors attribute to the formation of magnetite-allanite aggregates. The International Mineralogical Association distinguishes between three types of minerals depending on dominating REEs: allanite-(Ce), allanite-(La) and orthite-(Y). Besides orthite, the ores contain minerals of belovite-briolite, fluorite, uranothorianite, albite and amphibole. In addition, there are other minerals with REEs, such as xenotime, euxenite or priorite [8].

A small content of REEs, their scattered presence in ores and a large amount of thorium impede the industrial processing of orthite. Nevertheless, allanite can be considered as a useful promising resource for REE production, because it is widely available and can be processed according to the technologies used for monazite with small improvements [9,10]. However, it is possible to obtain significant amounts of orthite from the extraction of other minerals.

Currently, there are several deposits that potentially can be the sites of the allanite extraction: the uranium tailings storage facility in Queensland (Australia), the surveyed area Alice Springs in Australia's Northern Territory (1 mln tons of ore, 4% of orthite, 20% of rare-earth oxides) and deposits in the Hall Mountain Group in Idaho, USA [2].

In Russia, there are also orthite deposits. Orthite grains are often found in small amounts when investigating the mineral composition of different deposits [3,11–13]. Orthite is noted to belong to a strongly electromagnetic subfraction. It is also highly radioactive. The mineral contains up to 5.60% of ThO_2 (thororthite) and up to 0.1% of U_3O_8. Orthite, being a species of talcose and rare-earth pegmatites of high-temperature origin (found in Middle Asia, Norway, Sweden, North Carolina, PRC and other regions), is enriched with heavy lanthanides (Sm, Gd), yttrium, thorium and uranium (Table 1) [14].

Table 1. Relation of cerium REEs to yttrium REEs and thorium to uranium in orthites.

Deposit	Ce/Y	Content [wt%]		Th/U
		Th	U	
Th/U	6.04	0.60	0.040	15.0
Alakurtti, Karelia (pegmatite)	5.7	1.10	0.071	15.5
Koita-Tundra (pegmatite)	10.1	1.75	0.230	7.6
Khetolambina (pegmatite)	49	1.20	0.025	41.3
Ilmensky Mountains (pegmatite)	80	1.40	0.016	88.0
Vishnevy Mountains (pegmatite)	200	0.40	0.001	400

The content of radioactive elements in orthite is poorly studied. The data on the forms of uranium and thorium in orthites are also scarce. Radioactive elements are supposed to be present in orthite not only as an isomorphic impurity, but also as independent minerals, which provides prerequisites for enrichment of orthite by physical methods and separation of a considerable part of radioactive impurities. The processing of allanite may allow considerably expanding the raw material base of REEs. This makes the study of the content and forms of the radioactive elements in orthite (allanite) topical.

2. Materials and Methods

The work studies the specimens of orthite (allanite) ores obtained in the Vernadsky mine (Slyudyanka River, Irkutsk region) and the Yuzhno-Bogatyrskoye occurrence (Kuznetsk Alatau).

The elemental chemical composition of the ore was determined by electronic microscopy of the specimen's surface using the Hitachi S-3400N (Hitachi Ltd., Tokyo, Japan) microscope equipped with the Bruker (MA, USA) attachment for energy-dispersive analysis that allows determining the content of chemical elements obtained from Li to U starting with 0.1%–0.5%. It also allows studying their spatial distribution in the matrix under investigation. The analyses (TEM studies, SEM research, EBSD analysis and microstructure investigations) were carried out using the equipment of the Tomsk Regional Core Shared Research Facilities Center of National Research Tomsk State University.

The instrumental neutron activation analysis (INAA) was performed in the certified (certificate #ROSS RU.0001.511901) nuclear-geochemical laboratory of Tomsk Polytechnic University (Tomsk, Russia) at the research nuclear reactor facility "IRT-T" using certified methods (NSAM VIMS #410-YaF).

3. Results

3.1. Forms of Uranium and Thorium in Orthite Obtained from the Vernadsky Mine (Slyudyanka River)

The appearance of orthite obtained from the Vernadsky mine is shown in Figure 1. The length of the ore pieces is 5–6 cm.

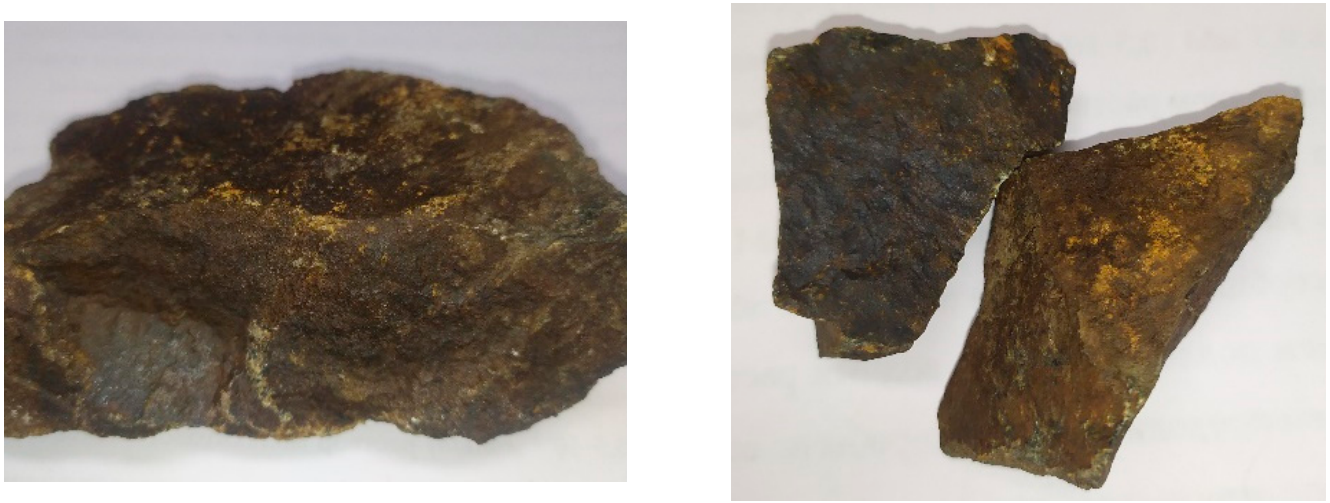


Figure 1. Appearance of orthite obtained from the Vernadsky mine.

The analysis of the defectless part of the crystal of the obtained materials (Figures 2 and 3, Table 2) shows that the concentrations of La and Ce are close, i.e., 6.59% and 7.01%, respectively, which is not typical. The content of Th is 2.61%, while that of U is below the detection threshold (0.1%).

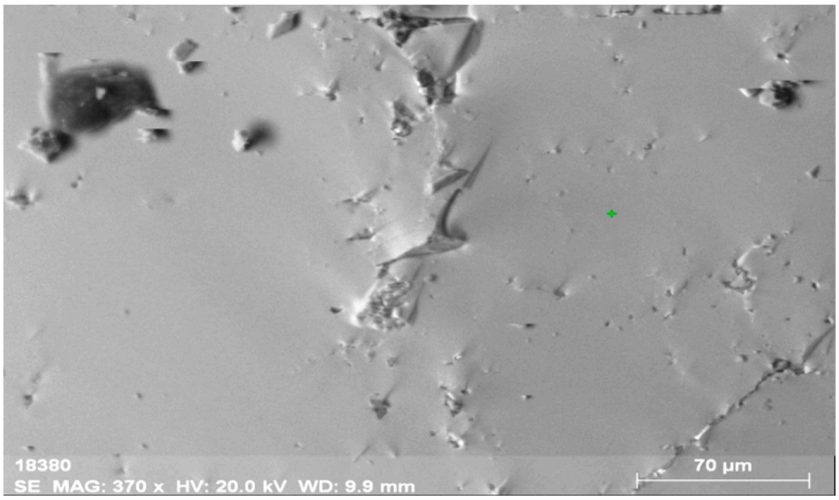


Figure 2. General view of the surface of orthite obtained from the Vernadsky mine. The surface has few defects and no mineral inclusions.

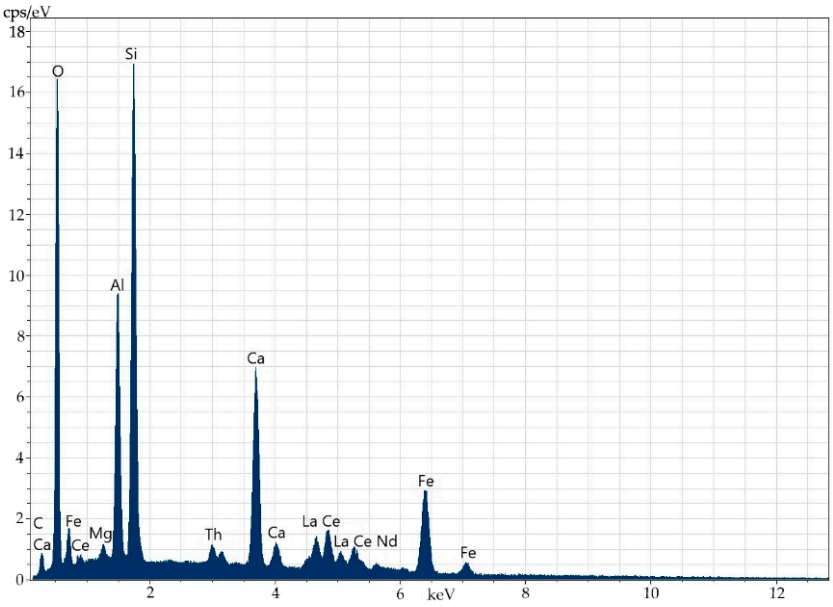


Figure 3. Energy-dispersive spectrum of the elements in the entire surface of the specimen.

Table 2. Mineral composition (wt%) of the surface.

Element	AN	Series	Net	[wt%]	[norm.wt%]	[norm.at.%]	Error [%]
Carbon	6	K-series	5091	1.550	1.567	3.335	0.276
Oxygen	8	K-series	127,628	39.030	39.442	63.031	4.365
Magnesium	12	K-series	7497	0.813	0.822	0.865	0.073
Aluminum	13	K-series	96,815	8.210	8.297	7.862	0.419
Silicon	14	K-series	187,547	11.997	12.124	11.037	0.537
Calcium	20	K-series	106,722	9.042	9.138	5.830	0.290
Iron	26	K-series	59,241	10.802	10.916	4.998	0.317
Lanthanum	57	L-series	41,331	6.526	6.594	1.214	0.275
Cerium	58	L-series	42,292	6.934	7.008	1.279	0.364
Neodymium	60	L-series	8211	1.468	1.484	0.263	0.250
Thorium	90	M-series	17,109	2.580	2.608	0.287	0.112

The composition of the main orthite matrix is nearly uniform along the entire surface of the mineral. This fact is related to main matrix elements (Al, Si, Ca, Fe), REEs (Ce, La, Nd) and Th. Sometimes, Ti occurs on the periphery of the mineral (up to 0.6%). The distribution of the elements is very uniform, which allows introducing the isomorphic inclusion of thorium into the crystalline structure of the mineral.

Oftentimes, along the basal planes and in cracks, there are finely dispersed mineral phases of separate thorium (Figures 4 and 5, Table 3) and uranium-thorium minerals (Figures 6 and 7, Table 4) without REEs in them. These phases include radiogenic lead (up to 2.9%).

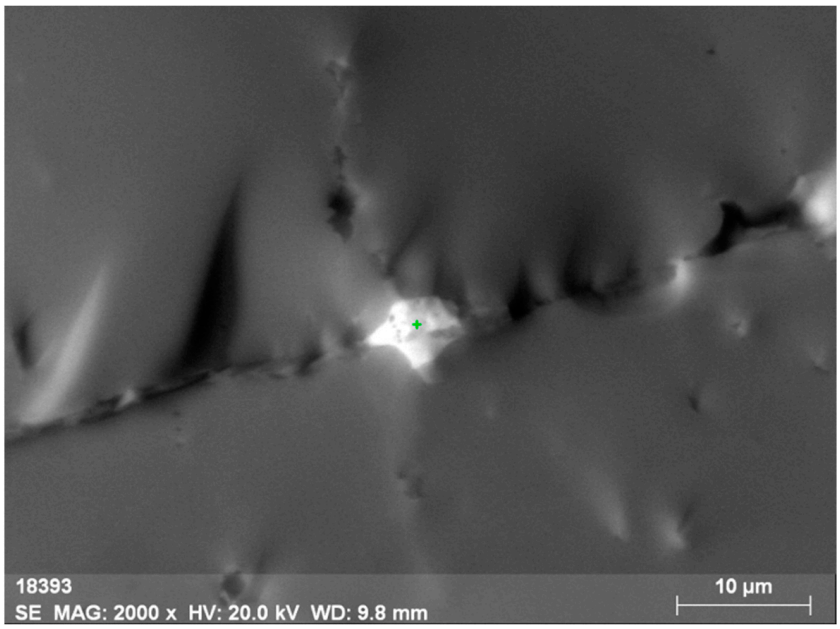


Figure 4. Micromineral phase of thorianite (ThO_2) intersecting orthite.

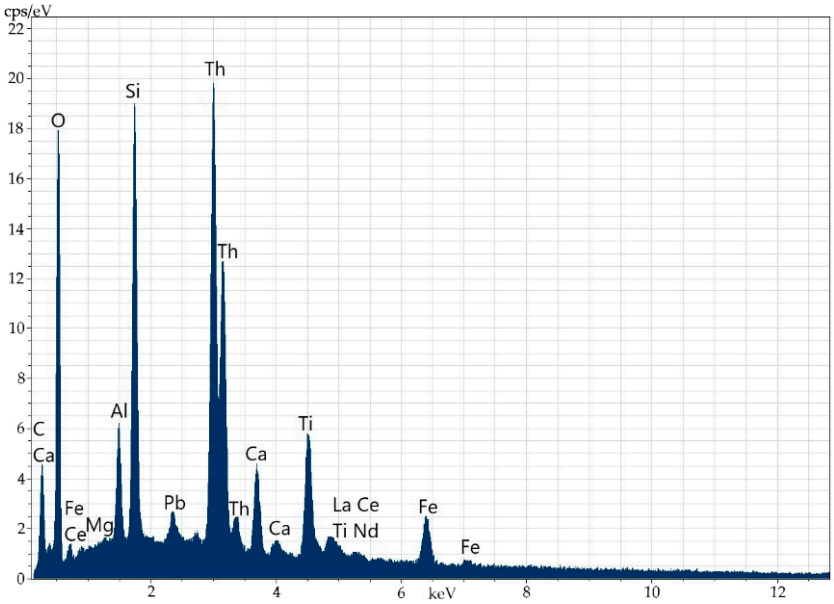


Figure 5. Energy-dispersive spectrum of the thorianite micromineral.

Table 3. Elemental composition (wt%) of the micromineral (Th, Pb, O).

Element	AN	Series	Net	[wt%]	[norm.wt%]	[norm.at.%]	Error [%]
Carbon	6	K-series	10,398	8.242	6.837	16.407	1.191
Oxygen	8	K-series	43,094	43.331	35.944	64.756	19.022
Magnesium	12	K-series	1383	0.252	0.209	0.248	0.043
Aluminum	13	K-series	15,062	2.097	1.739	1.858	0.128
Silicon	14	K-series	59,880	5.822	4.829	4.956	0.315
Calcium	20	K-series	18,848	3.367	2.793	2.009	0.128
Iron	26	K-series	11,497	3.140	2.605	1.344	0.117
Lanthanum	57	L-series	6397	1.894	1.571	0.326	0.146
Cerium	58	L-series	7172	2.157	1.789	0.368	0.142
Neodymium	60	L-series	597	0.189	0.157	0.031	0.118
Lead	82	L-series	1944	3.444	2.857	0.397	0.185
Thorium	90	M-series	146,378	40.321	33.447	4.155	1.305
			Sum	120.552	100.000	100.00	

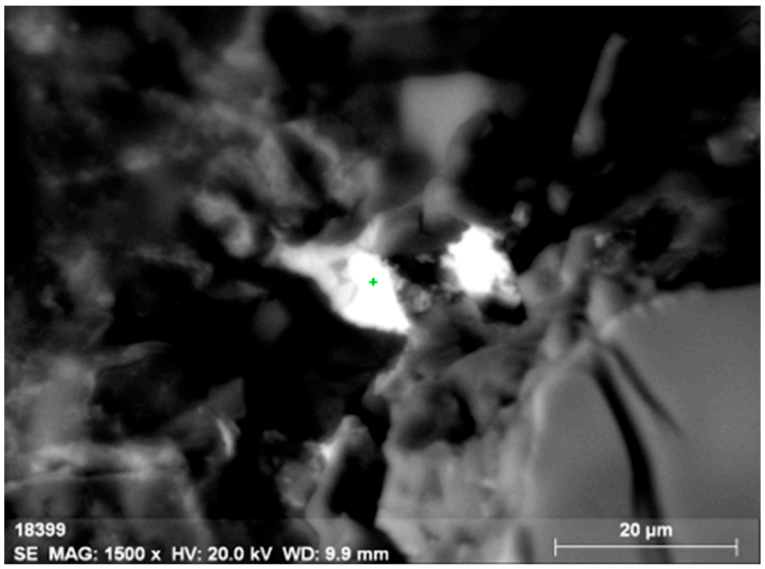


Figure 6. Microinclusion of uranothorianite (up to 1.9% of uranium) in orthite.

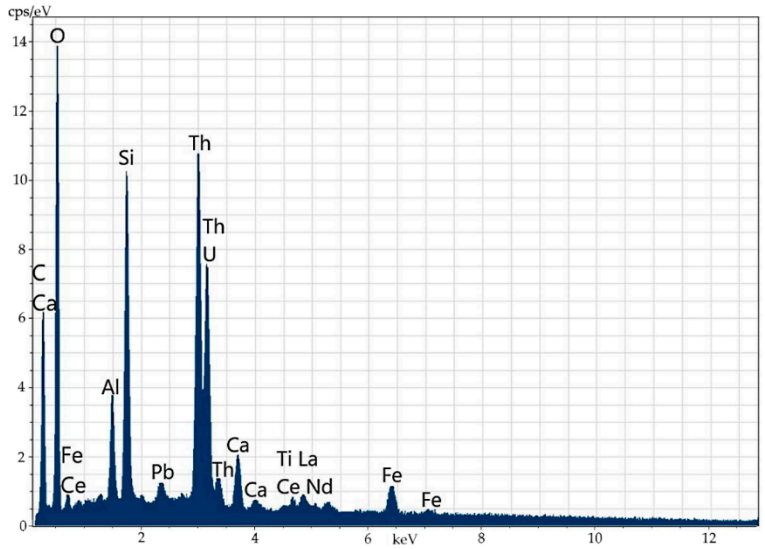


Figure 7. Energy-dispersive spectrum of the uranothorianite microinclusion in orthite.

Table 4. Elemental composition (wt%) of the uranothorianite micromineral.

Element	AN	Series	Net	[wt%]	[norm.wt%]	[norm.at.%]	Error [%]
Carbon	6	K-series	16,904	15.726	13.707	26.869	2.106
Oxygen	8	K-series	37,771	46.260	40.320	59.337	21.282
Magnesium	12	K-series	1463	0.475	0.414	0.401	0.058
Aluminum	13	K-series	13,269	3.340	2.911	2.541	0.190
Silicon	14	K-series	39,592	7.166	6.245	5.236	0.401
Calcium	20	K-series	9210	2.195	1.913	1.124	0.100
Iron	26	K-series	6642	2.212	1.928	0.813	0.094
Lanthanum	57	L-series	3566	1.468	1.279	0.217	0.209
Cerium	58	L-series	4514	1.800	1.569	0.264	0.170
Neodymium	60	L-series	654	0.251	0.219	0.036	0.126
Lead	82	L-series	1533	2.666	2.324	0.264	0.154
Thorium	90	M-series	85,429	28.611	24.937	2.530	1.370
Uranium	92	M-series	5880	2.131	1.858	0.184	0.249
			Sum	114.734	100.000	100.00	

3.2. Radioactive Elements and Their Forms in the Ore of the Yuzhno-Bogatyrskoye Occurrence (Kuznetsk Alatau)

Orthite is the most widely spread mineral in the specimens under study: its content is 90%–96%. According to the polished sections, orthite can be classified into two groups. The orthite of the first generation is represented by isometric or elongated crystals with a length-to-width ratio of 2:1 and 3:1. The crystals with the prismatic habitus in the cross-section resemble hexagonal prisms. The color is nonuniform; the internal parts of the grains and crystals feature pleochroism in darker shades; the external parts have lighter green-brownish shades. Presumably, the central parts have preserved the patterns of the previously replaced mineral, while the boundary ones are orthite new separate formations.

After the second stage of metasomatosis, orthite changes. The polished sections evidently differ from the first-generation orthite by the light-brownish color along with pleochroism present in brownish shades. This generation occurs together with fluorite and other minerals of this association.

The sand fraction of the specimen includes black, brownish-black, brownish and violet-black orthite. The latter is colored by the microinclusions of fluorite. Evidently, black and brownish-black orthite, whose content reaches 64.5% of the entire sand fraction mass, is nonuniform and is related to orthite of both first and second generations. Brownish orthite, whose content amounts to 27%, belongs to the first generation. The main accumulation of brownish orthite occurs in the fraction class of –0.5 + 0.25 mm (10.76%); the maximum concentration of black orthite is in the fraction class of –2.0 + 0.5 mm (30.77%).

INAA was used to analyze orthites of different colors. The analysis results are presented in Table 5, which demonstrates that the maximum concentration of REEs and thorium (up to 0.21%) is associated with the darkest varieties of orthite; however, the maximum concentration of heavy lanthanides is noted in brownish orthites. The content of uranium is determined only in brownish-black varieties, where it amounts to 166 g/t.

Electron microscopy fairly well confirms the polymineral character of the specimen, which is a fine mixture of orthite and rock-forming minerals (feldspars, amphiboles, quartz, fluorite and others). There are several types of orthite: thorium-less yttrium-containing orthite with REEs (Figures 8 and 9, Table 6) and yttrium-thorium-containing REE-less orthite with the thorium content of up to 6% (Figures 10 and 11, Table 7).

Table 5. Content of the elements (g/t) in the specimen minerals (INAA results).

Element	Fluorite	Orthite			
		Brownish	Brownish-Black	Black	Violet-Black
Fe	* N.D.	* N.D.	20795	27015	77416
Co	19	16	12	11	24
La	1402	11540	11760	8190	6230
Ce	2840	17014	16827	11931	32524
Sm	179	581	556	364	297
Eu	60	459	431	267	
Tb	13	110	105	69	127
Yb	90	327	331	222	235
Lu	14	45	54	37	44
Ag	502	48	42	-	110
Th	1889	1152	1218	896	2183
U	* N.D.	* N.D.	166	*N.D.	*N.D.

* N.D. = not detected.

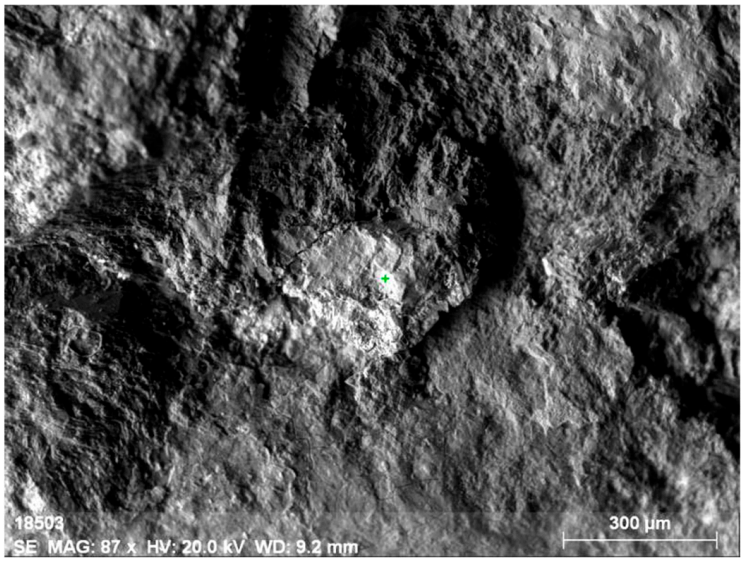


Figure 8. Thorium-less yttrium-containing orthite with REEs.

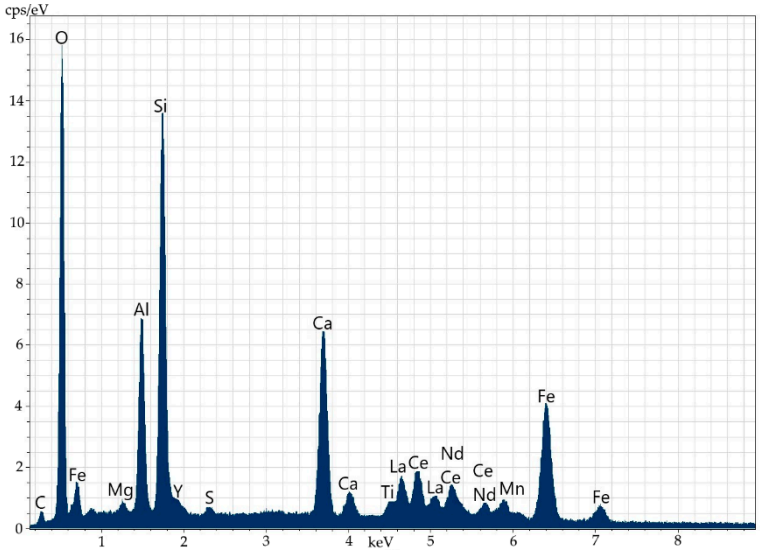


Figure 9. Energy-dispersive spectrum of thorium-less yttrium-containing orthite with REEs.

Table 6. Elemental composition (wt%) of thorium-less yttrium-containing orthite with REEs.

Element	AN	Series	Net	[wt%]	[norm.wt%]	[norm.at.%]	Error [%]
Carbon	6	K-series	2096	1.276	1.268	2.661	0.272
Oxygen	8	K-series	69,357	41.448	41.182	64.886	15.560
Magnesium	12	K-series	3089	0.715	0.711	0.737	0.070
Aluminum	13	K-series	40,490	7.309	7.262	6.784	0.378
Silicon	14	K-series	88,603	11.930	11.853	10.639	0.539
Calcium	20	K-series	58,598	7.402	7.354	4.626	0.244
Titanium	22	K-series	4962	0.814	0.810	0.426	0.067
Manganese	25	K-series	7634	1.631	1.621	0.744	0.173
Iron	26	K-series	47,595	11.737	11.661	5.263	0.344
Yttrium	39	L-series	4258	1.209	1.201	0.340	0.089
Lanthanum	57	L-series	25,403	5.723	5.687	1.032	0.266
Cerium	58	L-series	29,611	6.881	6.837	1.230	0.370
Neodymium	60	L-series	9040	2.269	2.254	0.394	0.330
			Sum	100.647	100.000	100.00	

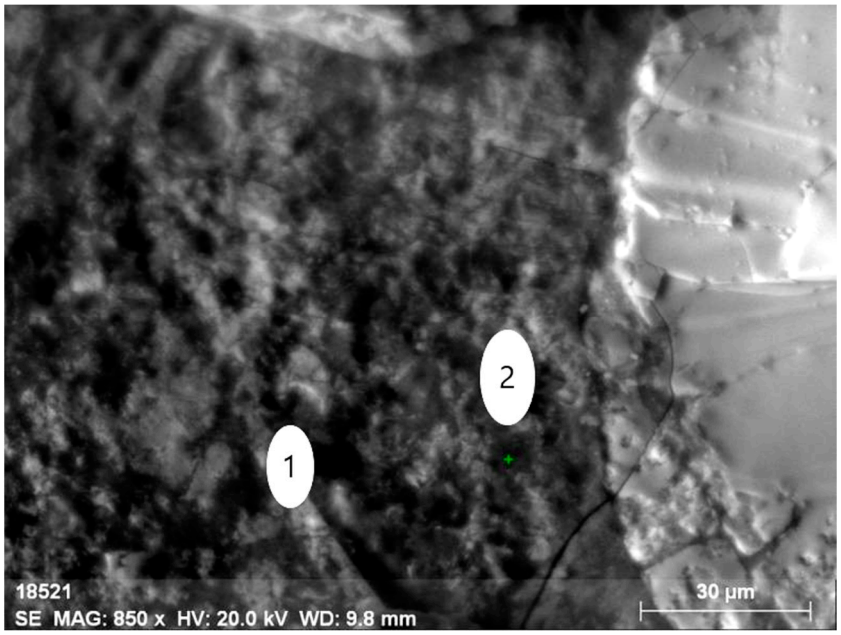


Figure 10. Mineral aggregate comprising yttrium-containing orthite with (1) the low content of REEs (dark grey) and (2) the thorianite aggregate (grey).

Table 7. Elemental composition (wt%) of orthite at point 1.

Element	AN	Series	Net	[wt%]	[norm.wt%]	[norm.at.%]	Error [%]
Carbon	6	K-series	3932	1.432	1.584	2.670	0.267
Oxygen	8	K-series	170,310	56.267	62.542	79.112	6.226
Magnesium	12	K-series	5751	0.435	0.481	0.401	0.050
Aluminum	13	K-series	73,835	4.537	5.020	3.765	0.243
Silicon	14	K-series	195,491	9.556	10.573	7.619	0.434
Calcium	20	K-series	46,964	3.879	4.292	2.167	0.140
Iron	26	K-series	44,151	6.376	7.054	2.556	0.197
Yttrium	39	L-series	7882	0.865	0.957	0.218	0.278
Thorium	90	M-series	37,255	5.437	6.016	0.525	0.198
			Sum	90.381	100.000	100.00	

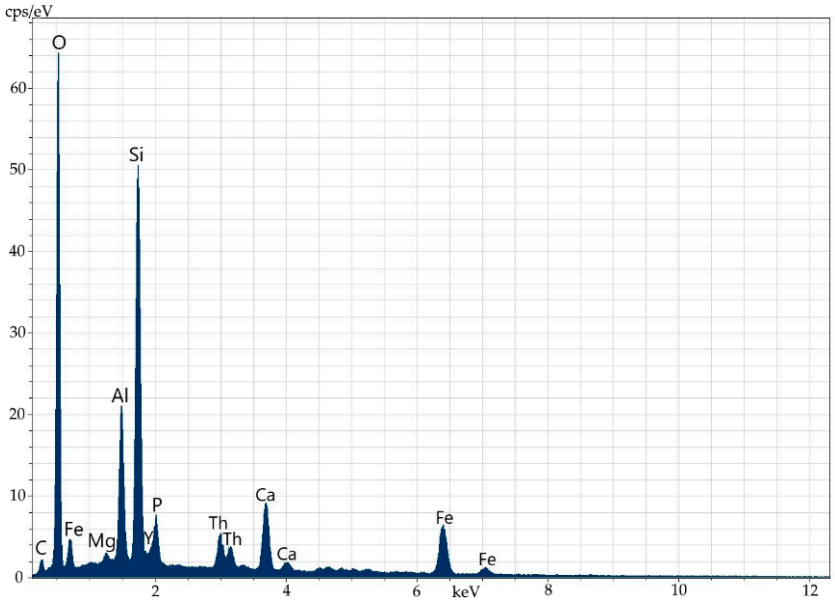


Figure 11. Energy-dispersive spectrum of orthite at point 1.

In this way, one can conclude that the main mass of orthite of the studied ores does not contain an appreciable amount of thorium (the detection threshold of 0.2% is below). The same can be claimed about uranium. The major amount of thorium in these ores is contained as a separate phase. It can be present in a close concretion with orthite (Figure 12, Table 8) or it often forms clearly distinguished microstreaks in orthite (Figures 13 and 14, Table 9). Electronic microscopy has not detected uranium mineral phases in ores, including orthite; however, their presence can be testified by fission radiography (Figure 15).

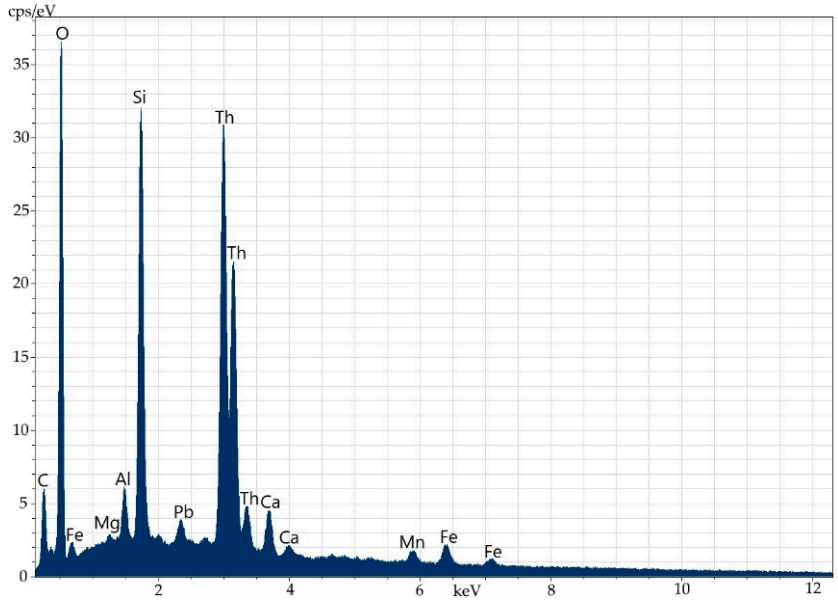


Figure 12. Energy-dispersive spectrum of thorium at point 2.

Table 8. Elemental composition (wt%) of thorium at point 2.

Element	AN	Series	Net	[wt%]	[norm.wt%]	[norm.at.%]	Error [%]
Carbon	6	K-series	13,662	5.789	5.254	11.432	0.815
Oxygen	8	K-series	116,604	51.535	46.773	76.400	5.793
Magnesium	12	K-series	1252	0.081	0.073	0.079	0.030
Aluminum	13	K-series	14,116	0.762	0.691	0.670	0.062
Silicon	14	K-series	141,401	5.873	5.329	4.959	0.293
Calcium	20	K-series	22,774	1.838	1.668	1.088	0.080
Manganese	25	K-series	7494	0.889	0.806	0.384	0.051
Iron	26	K-series	11,864	1.620	1.470	0.688	0.071
Lead	82	L-series	2444	2.085	1.893	0.239	0.119
Thorium	90	M-series	327,017	39.707	36.037	4.059	1.270
			Sum	110.182	100.000	100.00	



Figure 13. Mineral phase of thorianite shown as a streak in orthite.

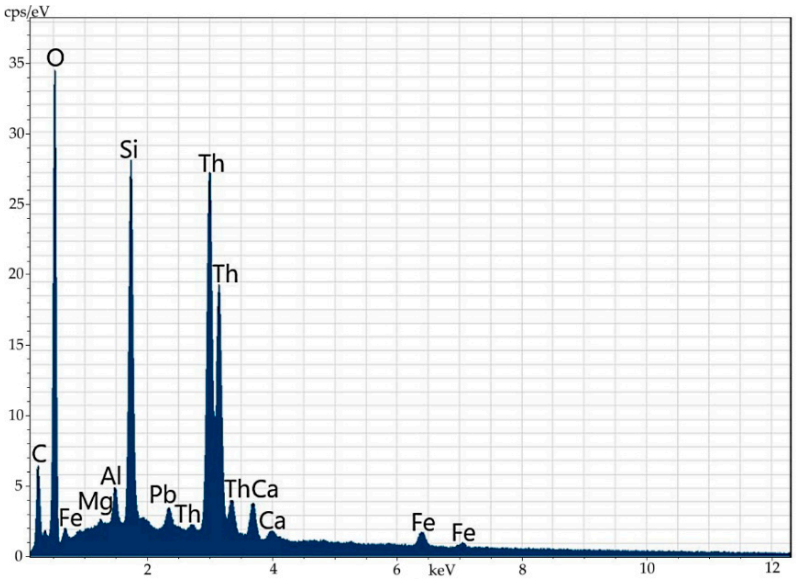
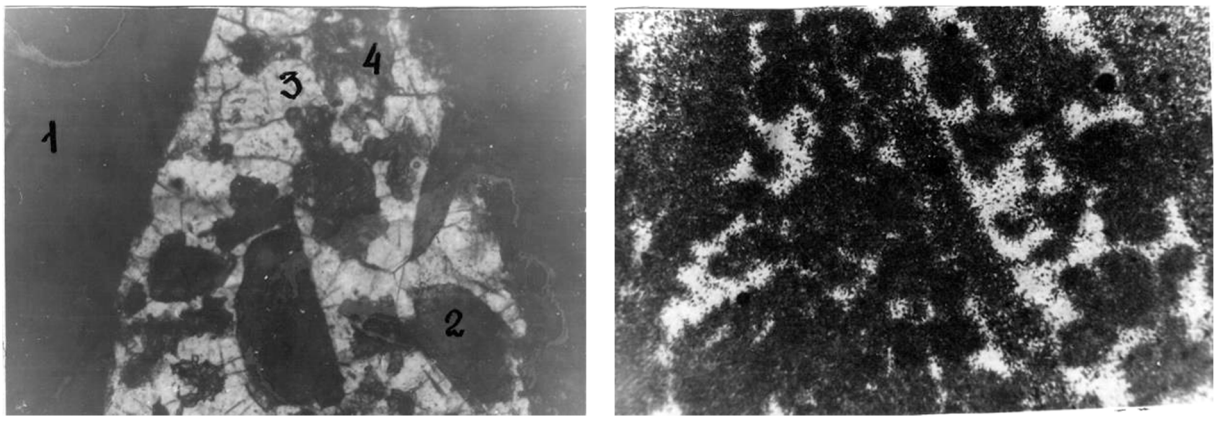


Figure 14. Energy-dispersive spectrum of the mineral phase of thorianite shown as a streak in orthite.

Table 9. Elemental composition (wt%) of the mineral phase of thorianite shown as a streak in orthite.

Element	AN	Series	Net	[wt%]	[norm.wt%]	[norm.at.%]	Error [%]
Carbon	6	K-series	32,744	6.774	6.068	12.736	0.861
Oxygen	8	K-series	246,444	54.184	48.536	76.481	5.880
Magnesium	12	K-series	2226	0.069	0.062	0.064	0.029
Aluminum	13	K-series	24,082	0.641	0.574	0.536	0.056
Silicon	14	K-series	275,099	5.667	5.076	4.557	0.276
Calcium	20	K-series	43,812	1.809	1.620	1.019	0.079
Iron	26	K-series	21,308	1.476	1.322	0.597	0.066
Lead	82	L-series	3413	1.459	1.307	0.159	0.088
Thorium	90	M-series	642,033	39.556	35.433	3.850	1.261
			Sum	111.638	100.000	100.00	



(**a**) (**b**)

Figure 15. Distribution of uranium in the quartz-fluorite-orthite ore: (**a**) polished section, where nicols are parallel, 1, 2—orthite, 3—quartz, 4—fluorite; (**b**) fission radiography, dark areas correspond to microinclusions of uranium minerals.

For this reason, the orthite ores of the Yuzhno-Bogatyrskoe occurrence can theoretically be subjected to gravity concentration processes (for example, jigging, concentration on centrifugal concentrators, etc.) due to the higher density of thorium and uranium minerals (from 4.5 g/cm^3 and higher) compared to allanite (up to 4.2 g/cm^3 and often below this value). Flotation and magnetic separation [7] are also available for this ore. Thorium and uranium present in orthite in the form of an isomorphic impurity can be removed only by chemical or extraction methods.

4. Discussion

This study shows that the radioactive elements in orthite obtained from the Vernadsky mine are thorium and, evidently, uranium, being mainly an isomorphic inclusion in the orthite crystal lattice. A part of thorium and uranium is contained in the form of separate minerals: thorianite and uranothorianite.

Uranium and thorium in the orthite ores of the Yuzhno-Bogatyrskoye occurrence are mainly represented by their separate minerals, while the content of the orthite phase in the form of their isomorphic inclusion is small.

The Vernadsky Mine orthite can be assumed to be the first-generation orthite, which explains its thorium content as an isomorphic impurity. On the contrary, the Yuzhno-Bogatyrskoye occurrence is partially altered. The separation of radioactive elements from the orthite and their formation of independent minerals can be explained by the process of metasomatosis, in particular, greisenization.

The obtained results are consistent with the literature data. For example, Wood S.A. and Ricketts A. studied allanite-(Ce) in the Eocene Casto granite of Idaho [15]. Allanite with

signs of alteration was surrounded by grains of thorianite, and the most altered allanite was replaced by bastensite and thorianite.

The obtained results allow assuming that the major part of the radioactive inclusions in the Ortite ores of the Yuzhno-Bogatyrskoye occurrence can be removed during ore beneficiation.

Author Contributions: V.I.S. and R.A.N. have conceived the idea and planned the experiment; all authors have obtained the data; R.O.M., P.S.S., V.S.S., D.I.L. and D.A.B. have analyzed the data; I.V.A. has written the manuscript: A.S.S. has corrected the manuscript. All authors have read and agreed to the published version of the manuscript.

Funding: This study was supported by the Tomsk State University Development Programme (Priority-2030). This work was carried out with the financial support from the Ministry of Education and Science of the Russian Federation (State assignment No. FSWM-2020-0028).

Data Availability Statement: The authors confirm that the data supporting the results of this study are available in the article.

Acknowledgments: The research was carried out using the equipment of the Tomsk Regional Core Shared Research Facilities Center of the National Research Tomsk State University. The Center was supported by the Ministry of Science and Higher Education of the Russian Federation, Grant no. 075-15-2021-693 (no. 13.RFC.21.0012)).

Conflicts of Interest: The authors declare no conflict of interest.

References

1. Gupta, C.K.; Krishnamurthy, N. Extractive metallurgy of Rare Earths. *Int. Mater. Rev.* **1992**, *37*, 197–248. [CrossRef]
2. Sofronov, V.L.; Drozdetskaya, N.V.; Buynovskiy, A.S. Calculation of orthite thermodynamic properties at 298–423 K. In Proceedings of the VIIth Science and Technology Conference of the SCC, Seversk, Russia, 22–25 October 2002; pp. 214–220.
3. Osovetskiy, B.M. Rare-earth and tantalum-niobium mineralization of Mesozoic-Cenozoic sediments of Vyatsko-Kamskaya depression. *Litosfera* **2010**, *2*, 62–76.
4. Faiziev, A.R. Peculiarities in the distribution of uranium and thorium in enclosing rock of multi-metal (AG, PB, U, Cu, Bi, Zn, F) Bolshoy Kanimansur deposit. *Geokhimiya* **2007**, *129*, 52–67.
5. Arbuzov, S.I.; Rikhvanov, L.P. *Geochemistry of Radioactive Elements*; Tomsk Polytechnic University Press: Tomsk, Russia, 2010; p. 300, ISBN 978-5-89298-587-5.
6. Gieré, R.; Sorensen, S.S. Allanite and other REE-rich epidote-group minerals. *Rev. Mineral. Geochem.* **2004**, *56*, 431–493. [CrossRef]
7. Tzifas, I.T.; Papadopoulos, A.; Misaelides, P.; Godelitsas, A.; Göttlicher, J.; Tsikos, H.; Hatzidimitriou, A. New insights into mineralogy and geochemistry of allanite-bearing Mediterranean coastal sands from Northern Greece. *Geochemistry* **2019**, *79*, 247–267. [CrossRef]
8. Catlos, E.J.; Sorensen, S.S.; Harrison, T.M. Th-Pb ion-microprobe dating of allanite. *Am. Mineral.* **2000**, *85*, 633–648. [CrossRef]
9. Galata, A.A.; Kairov, E.E.; Muslimova, A.V.; Novikova, S.L.; Shamin, V.I. Study of sulfuric acid processing of orthite. In Proceedings of the Actual Problems of Innovative Development of Nuclear Technologies: Scientific Session of NRNU MEPhI, Seversk, Russia, 10–14 April 2017; pp. 20–21.
10. Avramchik, A.N.; Andrienko, O.S.; Anufrieva, S.I.; Afanasyev, N.I.; Baitasov, K.M.; Baitasov, M.A.; Vardan, G.A.; Daibova, E.B.; Dement, T.V.; Duisebayev, B.O.; et al. *Modern Technologies of Rare Metal and Rare Earth Industry*; Leontiev, L.I., Sachkov, V.I., Eds.; NTL: Tomsk, Russia, 2016; pp. 30–43, ISBN 978-5-89503-586-3.
11. Elokhin, V.A. Endogenic molybdenum-containing rare-earth formations of Ural. *Litosfera* **2009**, *3*, 47–63.
12. Udoratina, O.V. Minerals of rare-earth deposits of polar Ural. *Vestnik* **2008**, *2*, 17–20.
13. Buynovskiy, A.S.; Korotkevich, V.M.; Ryabov, A.S.; Kruglov, S.N. Project for creating an enterprise for producing individual REE on the basis of yttrium-orthite deposit "Bogatyryok". *Russ. Phys. J.* **2000**, *53*, 10–19.
14. Nozhkin, A.D.; Mustafin, V.Z. Ortite from the Yenisei Ridge. *Izv. Tomsk. Politekh. Inst.* **1964**, *127*, 75–89.
15. Wood, S.A.; Ricketts, A. Allanite-(Ce) from the Eocene Casto granite, Idaho: Response to hydrothermal alteration. *Can. Mineral.* **2000**, *38*, 81–100. [CrossRef]

Disclaimer/Publisher's Note: The statements, opinions and data contained in all publications are solely those of the individual author(s) and contributor(s) and not of MDPI and/or the editor(s). MDPI and/or the editor(s) disclaim responsibility for any injury to people or property resulting from any ideas, methods, instructions or products referred to in the content.